

Transmittance and optical constants of Eu films from 8.3 to 1,400-eV

Mónica Fernández-Perea, Manuela Vidal-Dasilva, José A. Aznárez, Juan I. Larruquert^{a)}, José

A. Méndez

GOLD-Instituto de Física Aplicada-Consejo Superior de Investigaciones Científicas

Serrano 144, 28006 Madrid, Spain

Luca Poletto, Denis Garoli

Istituto Nazionale per la Fisica della Materia-CNR & Dep. of Information

Engineering, Padua, Italy

A. Marco Malvezzi

Dipartimento di Elettronica, Università di Pavia and CNISM, Via Ferrata, 1, I27100 Pavia, Italy

Angelo Giglia, Stefano Nannarone

Laboratorio TASC-INFN-CNR, S.S. 14, km 163.5 in Area Science Park, I-34012 Trieste, Italy

ABSTRACT

The optical constants of Eu films were obtained in the 8.3-1,400 eV range from transmittance measurements performed at room temperature. Thin films of Eu were deposited by evaporation in ultra high vacuum conditions and their transmittance was measured *in situ*. Eu films were deposited onto grids coated with a thin, C support film. The refractive index n of Eu was calculated using the Kramers-Kronig analysis. Data were extrapolated both on the high- and low-energy sides by using experimental and calculated extinction coefficient values available in the literature. Eu, similar to other lanthanides, has a low-absorption band just below the O_{2,3} edge onset; the lowest absorption was measured at about 16.7 eV. Therefore, Eu is a promising material for filters and multilayer coatings in the energy range below the O_{2,3} edge in which materials typically have a strong

^{a)} Author to whom correspondence should be addressed. Electronic mail: larruquert@ifa.cetef.csic.es

absorption. The consistency of the composite optical constants was tested with the f and inertial sum rules and found to be good.

Keywords: Extreme Ultraviolet; Far Ultraviolet; Optical constants; Absorption filters; Multilayers; Optical properties of thin films

1. INTRODUCTION

Until recently, lanthanides had not been fully characterized in the extreme ultraviolet (EUV)-soft X-rays. However, an increased interest in these materials has grown with the recent characterization of La¹, Tb¹, Gd², Nd², Yb³, Ce⁴, and Pr⁵, and of materials with close chemical properties such as Sc^{6,7,8} and Y⁹. This paper addresses the optical properties of Eu films in the 8.3-1,400 eV range. The optical properties in this energy range are characterized by the high-energy tail of the valence electrons and by the presence of three intense absorption bands, O_{2,3}, N_{4,5}, and M_{4,5}, in order of increasing binding energy, due to the excitation of 5p, 4d, and 3d electrons above the Fermi level.

Scant data are available on the optical properties of Eu in the UV to soft X-rays. Zimkina *et al.*¹⁰ and Fomichev *et al.*¹¹ performed absorption measurements and provided data for the product of the absorption coefficient times the film thickness in the 95-520 eV and 100-115 eV ranges, respectively. However, these papers cannot be directly taken for absolute reference since the absorption coefficient cannot be deduced. Fischer and Baun¹² obtained absorption spectra of lanthanides and lanthanide oxides at the M_{4,5} edges; they only plotted the data for the oxides, and they doubted that their own measurements for Eu (not plotted) were characteristic of the metal. Thole *et al.*¹³ plotted absorption of lanthanide samples including Eu with focus on a small energy range in the region of the M_{4,5} edges aiming at line-shape analysis to determine the multiplet components contributing to the absorption peak; since the preparation of the samples is not clearly described and the ordinates in the plotted figures are not clear, the data can only be used qualitatively for the position of the absorption peaks. Bonnelle *et al.*¹⁴ reported shifts of x-ray absorption resonance lines from 1128.5 eV for Eu to 1131.2 and 1134.4 eV for Eu₂O₃. Mansfield and Connerade¹⁵ measured the absorption spectrum (in arbitrary units) of Eu vapor in the 131-153 eV range. Tracy¹⁶ obtained spectra of vapors of Eu and other lanthanides in the ~20-38 eV range, and

reported relative absorption cross-section plots. Müller¹⁷ measured reflectance of Eu films and other materials in the 0.3-5 eV range through sapphire windows on which an Eu film had been evaporated; the same author published conductivity data of Eu in the 0.3-4 eV range¹⁸. Endriz and Spicer¹⁹ measured the reflectance of Eu and other materials in the 1-11.5 eV range, and they deduced the dielectric constant and other functions in that range and extrapolated them down to 0.3 eV using Müller's data; their research was performed *in situ* in UHV conditions, with extreme care in handling the samples.

Other than optical measurements, Pétrakian²⁰ measured the conductivity of thin films of Eu and other materials in the 1.6-6.2 eV range. Brodén *et al.*²¹ reported the photoemission spectra and the absolute yield of films of Eu and other lanthanides. Trebbia and Colliex²² performed electron-energy-loss spectroscopy on Eu films that were deposited under a pressure of 1.33×10^{-4} Pa, but they were apparently exposed briefly to the atmosphere before being transferred to the microscope working at a pressure of 1.33×10^{-3} Pa; they obtained two peaks at 142 and 149 eV, respectively. Kaindl *et al.*²³ obtained the x-ray absorption through measurements of total electron yield of Eu₂O₃ at the Eu M_{4,5} edge. Electron-energy-loss spectroscopy in reflection mode was investigated by Netzer *et al.*²⁴. Kubo²⁵ calculated the energy band structure of Eu and Ba BCC metals and obtained their optical conductivity in the 0-10.5 eV range. Henke *et al.*²⁶ obtained a semi-empirical set of data in the 30-10,000-eV range (later extended to 30,000 eV²⁷). They could only use the experimental data of Ref. 10, which are not absolute because film thickness was not given.

This paper is aimed at providing accurate data on pure Eu samples over a broad spectral range. It is organized as follows. A brief description of the experimental techniques used is presented in Section 2. Section 3 presents transmittance data, extinction coefficient of Eu calculated from transmittance,

and dispersion obtained using Kramers-Kronig (K-K) analysis; the consistency of the data gathered in this research is also evaluated.

2. Experimental techniques

2.1 SAMPLE PREPARATION

Both Eu film deposition and characterization were performed *in situ* under UHV in two different facilities. Eu samples for the spectral range 22-1,400 eV were prepared and analyzed at the BEAR beamline of ELETTRA synchrotron (Trieste, Italy), and samples for the spectral range of 8.31-21.23 eV were prepared and analyzed at Grupo de Optica de Láminas Delgadas (GOLD) at Instituto de Física Aplicada-CSIC. Eu films were deposited onto thin C films supported on 117 mesh Ni grids with 88.6% nominal open area. The procedure for C film preparation was reported elsewhere⁸.

At BEAR beamline, Eu films were deposited with a TriCon evaporation source²⁸, in which a small Ta crucible is bombarded by electrons that impinge on the crucible wall. Eu chunks of 99.99 % purity from **LTS Chem. Inc.** were used. The crucible-sample distance was 200 mm. Deposition rate ranged from ~1.4 nm/min for the thinner films to ~3 nm/min for the thicker films. Film thickness was monitored with a quartz-crystal monitor during deposition. Witness glass substrates or Si substrates cut from Si wafers were placed close to the grid-supported C film and were coated with a similar Eu-film thickness. Reflectance *versus* the incidence angle was measured on the witness samples at optimum energies and the angular positions of the minima and maxima were used to calculate the Eu film thickness. Henke's optical constants²⁷ were used in this calculation. Henke's data were downloaded from the website of the Center for X-Ray Optics (CXRO) at Lawrence Berkeley National Laboratory²⁹. The distance between the area of transmittance measurements and that of reflectance measurements was ~10 mm.

At GOLD, Eu films were deposited by evaporation from Ta boats. The boat-sample distance was ~300 mm. Deposition rate was ~4.2 nm/min. Film thickness was monitored with a quartz-crystal monitor during deposition; those measurements were calibrated through Tolansky interferometry, i.e., through multiple-beam interference fringes in a wedge between two highly reflective surfaces³⁰.

Eu films both at BEAR and GOLD were deposited onto room-temperature substrates.

2.2 EXPERIMENTAL SETUP FOR TRANSMITTANCE MEASUREMENTS

At the BEAR beamline, measurements were performed with a vertical exit slit of 100 μm . With this configuration, the monochromator spectral broadening is of the order of 0.01 eV in the 22-100 eV range, 0.1 eV in the 100-500 eV range, and 1 eV in the 500-1,400 eV range. The suppression of higher orders was achieved using quartz, LiF, In, Sn, Al and Si filters at specific ranges below 100 eV, and choosing a plane-mirror-to-grating deviation angle in the monochromator setup that minimized higher-order contributions. The beam cross section at the sample was about $0.7 \times 1.5 \text{ mm}^2$.

The measurements were performed in the BEAR spectroscopy chamber³¹, connected in vacuum ($P=1.3 \times 10^{-8} \text{ Pa}$) to the preparation chamber, where *in situ* samples were prepared. Three C substrates were used. Three, one, and two successive Eu coatings were deposited upon the first, second, and third substrate, respectively, without breaking vacuum. Each sample was transferred back and forth between the deposition chamber and the measurement chamber, always under UHV, for the deposition of the successive Eu layers and their characterization.

For each film we evaluated the uniformity of the sample. The variation of transmittance signal at 140 eV was verified to be less than 0.5%. The sample was positioned for all the measurements in the same position within an uncertainty of 0.5 mm. We can estimate that the overall uncertainty in the

transmittance measurements is of the order of 2%. Possible fluctuations of the photon beam during transmittance measurements were recorded with a 100-V biased Au-mesh. These fluctuations were cancelled by normalizing the recorded beam intensity to the mesh current.

Transmittance measurements in the 8.31-21.2 eV were performed *in situ* at GOLD with a reflectometer that has been described elsewhere^{32, 33}. Three successive Eu coatings were deposited on a LiF substrate, and two coatings upon a C substrate, without breaking vacuum. Successive Eu coatings were deposited without breaking vacuum. The sample was transferred from the deposition to the characterization chamber after every deposition. Deposition, transfer and transmittance measurements were performed under UHV conditions.

In both facilities, transmittance measurements were performed on samples at room temperature.

3. Results and discussion

3.1 TRANSMITTANCE AND EXTINCTION COEFFICIENT OF Eu

We measured the transmittance of Eu films with the following thicknesses: 24, 41, 57, 58, and 94 (GOLD), 15, 18, 26, 33, 55, and 205 nm (BEAR). The transmittance of several Eu samples normalized to the transmittance of the uncoated substrate is plotted in Fig. 1. A low-energy band of relatively large transmittance with a peak at 16.7 eV was obtained. Close transmittance bands have been measured for other rare earths, as will be mentioned below. Eu, along with Yb, La, Tb, Ce, and Pr are promising materials for transmittance filters or multilayer spacers for the ~12-25-eV spectral range, where there has been a lack of low-absorbing materials until recently. In Fig. 1 there are three high-transmission bands peaked at ~1,100, 128.5 and 16.7 eV, right below the Eu M_{4,5}, N_{4,5}, and O_{2,3} edges, respectively.

If the contribution to transmittance coming from multiple reflections inside the Eu film is negligible, the extinction coefficient k (the imaginary part of the complex refractive index) can be calculated from transmittance with the following equation:

$$\ln\left(\frac{T_{fs}}{T_s}\right) \approx A - \left(\frac{4\pi k}{\lambda}\right)d \quad (1),$$

where T_s and T_{fs} represent the transmittance of the uncoated substrate and of the substrate coated with an Eu film, respectively; λ is the radiation wavelength in vacuum; d stands for the Eu film thickness. Eq. (1) is a straightforward result of the well-known Beer-Lambert law. A is a constant for each energy and encompasses the terms that involve reflectance, in the assumption that multiple reflections are negligible.

k of Eu films was calculated by fitting the slope of the logarithm of transmittance *versus* thickness at each energy using Eq. (1); the data are represented in Fig. 2. The data of Henke were calculated with a density of 5.25 g/cm³. No other data were found in the literature above 11.6 eV.

k at the O_{2,3} edge and both at and below the close low-absorption band are presented in Fig. 3, along with the data of Endriz and Spicer¹⁹. The smallest value of k is obtained at 16.7 eV, and the closest energies investigated were 14.87 and 18.45 eV. This minimum is closed to the ones obtained for other rare earths: La¹ at 16.5 eV, Ce⁴ at 16.1 eV, and Pr⁵ at 16.87 eV. The minima for the other investigated rare earths are at somewhat larger energies: Sc⁶ at 27 eV, Yb⁶ at 21.2 eV, Tb¹ at ~19.5 eV. k at the minimum amounts to 0.04 for Eu, which is the smallest value found for lanthanide minima except for Yb, which is, however, more absorbing than Eu at 16.7 eV. Optical properties of Eu in this range are then exceptional, and might be suitable for transmittance filters or for reflective multilayers. However, Eu is a very reactive material, and this may complicate its applicability for optical coatings.

Fig. 4 displays k around the Eu $N_{4,5}$ edge. The current data show a structure with a main peak at 141.5 eV and three secondary peaks at \sim 132.5, 134.0 and 136.0 eV; measurements every 0.5 eV are available here. The peaks are related to transitions from 4d to 4f shells. Fomichev *et al.*¹¹ reported secondary peaks at 132.3, 133.6, and 135.5 eV, which are between 0.2 and 0.5 eV below the present ones; they found two further and smaller peaks that are not found here. They did not measure the position of the main peak of Fig. 4. Mansfield and Connerade¹⁵ measured the absorption of Eu vapor and obtained a main peak at 140.6 eV, and three secondary peaks at 132.4, 133.7, and 135.4 eV. The latter 3 peaks are within 0.1 eV of those of Fomichev *et al.*¹¹.

k at the $M_{4,5}$ edge is presented in Fig. 5, along with experimental data of Thole *et al.*¹³ and the semiempirical data of Henke. Thole's data, not displaying any ordinate units, have been scaled to match the current peak heights. Two main peaks for Eu metal were obtained in the current research at 1129.8 ± 0.5 and 1158.0 ± 0.5 eV, and a secondary peak at 1133.8 ± 0.5 eV. Three similar peaks were measured at \sim 1.5 to 3.0 eV lower energy by Thole *et al.*¹³ Bonnelle *et al.*¹⁴ mentioned that Eu metal has a peak at 1128.5 eV, which is 1.3 eV lower energy than the present data. Tabulated data for the positions of M_5 and M_4 edges are 1130.9 and 1160.6 eV, respectively³⁴, which are at 1.1 and 2.6 eV larger energies than the current peaks, respectively. A peak was found at 1481.4 eV, and it is attributed to M_3 (1480.6 eV³⁴).

The uncertainty of the extinction coefficient was estimated in the following way: a computer code was used to add random errors to the experimental measurements; at every simulated measurement, transmittance and thickness values were randomly modified within the limits imposed by their relative uncertainties (0.02 in the case of transmittance and 0.05 in the case of thickness). With these modified values, the extinction coefficient was calculated in the usual way through the slope of the

logarithm of transmittance *versus* thickness. After a large number of measurement simulations, the standard deviation σ_k of the resulting set of extinction coefficient values was interpreted as δk , the uncertainty of k , with k taking values within $k \pm \delta k$. As a result of this procedure the relative uncertainty $\delta k/k$ of Eu extinction coefficient was determined to be between ~ 0.015 and ~ 0.025 in almost the whole spectral range, except for the interval 650 – 1150 eV, where the relative uncertainty increased up to a maximum value of ~ 0.06 . This increase in the relative uncertainty is due to the very small values of k in this spectral range.

3.2 REFRACTIVE INDEX CALCULATION THROUGH DISPERSION RELATIONS

The refractive index n of Eu was calculated using K-K dispersion relations:

$$n(E) - 1 = \frac{2}{\pi} P \int_0^{\infty} \frac{E' k(E')}{E'^2 - E^2} dE', \quad (2)$$

where P stands for the Cauchy principal value. The application of Eq. (2) to calculate n requires the availability of k data over the whole spectrum, so that we extended the present data with the available data in the literature and extrapolations. Between 1,400 and 3×10^4 eV we used Henke's data from the CXRO's web²⁹; these data along with the current measurements were coupled with a smooth connection. For even larger energies, the calculations of Chantler *et al.*³⁵ were used up to 1.7×10^5 eV. The extrapolation to infinity was performed by keeping constant the slope of the log-log plot of $k(E)$ of Chantler's data.

At energies smaller than the present measurements, we used the data of Endriz and Spicer¹⁹. Endriz and Spicer measured reflectance of Eu films in the 1-11.6 eV range. They calculated the optical constants of Eu in this range, which they extended down to 0.3 eV using the reflectance data of Müller¹⁷. However, Müller had measured the reflectance of Eu films through sapphire windows on

which an Eu film had been evaporated, so that Endriz and Spicer had to scale Müller's data in order to match the two sets. Endriz and Spicer developed a Drude model to extend the reflectance data down to 0 eV. A simple Drude model did not match well with the available data, and one of the parameters was allowed to linearly vary from 0 to 0.3 eV. We tried to follow this Drude model recipe, but we could not reproduce the parameters obtained by Endriz and Spicer for Eu. Furthermore, the extrapolation with Müller's data did not look very reliable, so we decided not to use Müller's data.

Instead, we operated in the following way. We extrapolated the Endriz-Spicer data from 1 to 0 eV with a new Drude model. In order to calculate Drude parameters, we used experimental data for the resistivity of Eu³⁶, from which we obtained conductivity $\sigma=1.01 \times 10^{16} \text{ s}^{-1}$ (CGS units), and of the experimental loss-function peak as displayed by Endriz and Spicer in their Table II, from which we obtained the free-electron plasma energy $E_p=\hbar\omega_p=8.66 \text{ eV}$. These parameters resulted in the electronic relaxation time of $\tau=7.33 \cdot 10^{-16} \text{ s}$. This Drude model did not reproduce the reflectance measured by Endriz and Spicer at 1 eV. Therefore in the interval 0-1 eV the values of E_p and τ were allowed to vary with energy according to linear or square root laws of the form $\tau(E) = \tau_0[1 - A(E/E_0)^{(1,0.5)}]$, $E_p(E) = E_{p0}[1 - B(E/E_0)^{(1,0.5)}]$, where $E_0=1 \text{ eV}$, and (1, 0.5) means that whichever of the two powers were tried. The linear variation of Drude parameters resulted in an abrupt connection with Endriz's reflectance at 1 eV (0.681), even though there were two free parameters (A and B) and one constraint (the reflectance at 1 eV). On the contrary, the variation of Drude parameters with the square root of energy resulted in a smoother connection at 1 eV, and this approach was adopted, which provided an extrapolation for k down to zero energy starting with the Endriz-Spicer data. Table 1 summarizes the parameters used in the Drude model.

Fig. 6 displays the k data of Eu that were assembled for the K-K analysis. Figs. 7 to 10 display $\delta=1-n$ calculated with Eq. (2) using data plotted in Fig. 6; n or δ at the O_{2,3}, N_{4,5}, and M_{4,5} edges is shown in Figs. 8, 9, and 10, respectively. Only Endriz-Spicer and Henke data are available for comparison.

3.3 CONSISTENCY OF OPTICAL CONSTANTS

The f sum rule relates the number density of electrons to k (or to other functions); it provides a guidance to evaluate the accuracy of k data. It is useful to define the effective number of electrons $n_{eff}(E)$ contributing to k up to given energy E :

$$n_{eff}(E) = \frac{4\varepsilon_0 m}{\pi N_{at} e^2 h^2} \int_0^E E' k(E') dE', \quad (3)$$

where N_{at} is the atom density, e is the electron charge, ε_0 is the permittivity of vacuum, m is the electron mass, and h is Planck's constant³⁷. The f sum rule expresses that the high-energy limit of the effective number of electrons must reach $Z=63$, i.e., the atomic number of Eu. When the relativistic correction on the scattering factors is taken into account, the high-energy limit of Eq. (3) is somewhat modified. The following modified Z was used: $Z^*=62.04$ ³⁸. The high-energy limit obtained here with Eq. (3) was 60.54, which is a 2.4% smaller than the above Z^* value. The main contribution to n_{eff} was found to come from the ~ 1 to 6×10^5 eV range. The difference with Z^* may be attributed to inaccuracies in the film thickness determination, in the k data used in the low energy extrapolation, in the transmittance measurements, and to a possible lower density of the film thickness compared to bulk density, which was used in N_{at} .

A useful test to evaluate the accuracy of K-K analysis is obtained with the inertial sum rule:

$$\int_0^{\infty} [n(E) - 1] dE = 0, \quad (4)$$

which states that the average of the refractive index throughout the spectrum is unity. The following parameter is defined to evaluate how close to zero the integral of Eq. (4)³⁷ is:

$$\zeta = \frac{\int_0^{\infty} [n(E) - 1] dE}{\int_0^{\infty} |n(E) - 1| dE} \quad (5)$$

Shiles *et al.*³⁷ suggested that a good value of ζ should stand within ± 0.005 . An evaluation parameter $\zeta = -0.0001$ was obtained with the inertial sum rule test. Therefore, the inertial sum rule test is well within the above top value, which, along with the above obtained result for the f sum rule, suggest good consistency of n and k data.

In order to check the validity of the modified Drude model that was applied in section 3.2, a test was performed through the following sum-rule³⁹:

$$\int_0^{\infty} [\varepsilon_1(\omega) - 1] d\omega = -2\pi^2 \sigma(0), \quad (6)$$

where ω , ε_1 and $\sigma(0)$ stand for the frequency, the real part of the dielectric constant, and the DC conductivity, respectively. With the current data, the main contribution to the integral of Eq. (6) was found in the spectral range ~ 0.001 -10 eV, and hence the sum-rule stresses the low-energy range. The sum-rule of Eq. (6) resulted in a DC conductivity 3.8% larger than the original value of Curry *et al.*³⁶ that was used in the above modified Drude model. From this reasonable agreement we conclude that the modified Drude model here used result in self-consistent optical-constant data.

CONCLUSIONS

The transmittance of thin films of Eu deposited by evaporation has been measured *in situ* in the 8.3-1,400 eV photon energy range under UHV conditions. The extinction coefficient of Eu has been

calculated from transmittance measurements in the same spectral range. Eu features a deep absorption minimum at ~ 16.7 eV, with k at this energy being lower than the one corresponding to all the other rare-earths investigated so far. This relatively low absorption at this spectral range makes Eu a promising candidate for transmittance filters and reflective multilayers. Given the high reactivity of Eu, a surface passivation method must be developed to prevent surface instability of Eu in contact with atmosphere.

The refractive index of Eu in the same range was obtained with K-K analysis over an extended spectral range.

Current data are the first experimental data of both the extinction coefficient and the refractive index of Eu in the whole spectral range investigated except the 8.3-11.6-eV range. The current data encompass the Eu $M_{4,5}$, $N_{4,5}$ and $O_{2,3}$ edges.

The evaluation of f and inertial sum rules shows good consistency of the optical constants of Eu.

ACKNOWLEDGMENTS

We acknowledge support by the European Community - Research Infrastructure Action under the FP6 "Structuring the European Research Area" Programme (through the Integrated Infrastructure Initiative "Integrating Activity on Synchrotron and Free-Electron-Laser Science"). This work was also supported by the National Programme for Space Research, Subdirección General de Proyectos de Investigación, Ministerio de Ciencia y Tecnología, project numbers ESP2005-02650, ESP2005-25299-E, and ESP2006-27266-E. A. M. M. acknowledges the partial support of the Fondo d'Ateneo per la Ricerca (FAR) of Università di Pavia. M. F. is thankful to Consejo Superior de Investigaciones Científicas (Spain) for funding under the Programa I3P (Ref. I3P-BPD2004), partially supported by the

European Social Fund. M. V. acknowledges financial support from a FPI BES-2006-14047 fellowship.

The technical assistance of J. M. Sánchez-Orejuela is acknowledged.

REFERENCES

1. Yu. Uspenski, J. Seely, N. Popov, I. Artioukov, A. Vinogradov, D. Windt, B. Kjornrattanawanich, “Extreme UV optical constants of rare-earth metals free from effects of air contamination”, in *Soft X-Ray Lasers and Applications VI*, E. E. Fill, ed., Proc. SPIE **5919**, 213-220 (2005).
2. B. Kjornrattanawanich, D. L. Windt, Y. A. Uspenskii, J. F. Seely, “Optical constants determination of neodymium and gadolinium in the 3 nm to 100 nm wavelength range”, in *Advances in X-ray/EUV optics, components, and applications*, A. M. Khounsary, C. Morawe, eds., Proc. of SPIE **6317**, 63170U (2006).
3. M. Fernández-Perea, J. I. Larruquert, J. A. Aznárez, J. A. Méndez, L. Poletto, D. Garoli, A. M. Malvezzi, A. Giglia, S. Nannarone “Determination of the transmittance and extinction coefficient of Yb films in the 23-1,700-eV range”, *J. Opt. Soc. Am. A* **24**, 3691-3699 (2007).
4. M. Fernández-Perea, J. I. Larruquert, J. A. Aznárez, J. A. Méndez, L. Poletto, D. Garoli, A. M. Malvezzi, A. Giglia, S. Nannarone “Determination of the transmittance and extinction coefficient of Ce films in the 6-1,200-eV range”, *J. Appl. Phys.* **103**, 073501-1 to -7 (2008).
5. M. Fernández-Perea M. Vidal-Dasilva, , J. A. Aznárez, J. I. Larruquert, J. A. Méndez, L. Poletto, D. Garoli, A. M. Malvezzi, A. Giglia, S. Nannarone “Determination of the transmittance and extinction coefficient of Pr films in the 4-1,600-eV range”, (submitted for publication.)
6. A. L. Aquila, F. Salmassi, E. M. Gullikson, F. Eriksson, J. Birch, “Measurements of the optical constants of scandium in the 50-1300 eV range”, in *Optical constants of materials for UV to x-ray wavelengths*, R. Soufli and J. F. Seely, eds., Proc. of SPIE **5538**, 64-71 (2004).
7. Y. A. Uspenskii, J. F. Seely, N. L. Popov, A. V. Vinogradov, Y. P. Pershin, and V. V. Kondratenko, “Efficient method for the determination of extreme-ultraviolet optical constants in reactive materials: application to scandium and titanium”, *J. Opt. Soc. Am. A* **21**, 298-305 (2004).

8. M. Fernández-Perea, J. I. Larruquert, J. A. Aznárez, J. A. Méndez, L. Poletto, A. M. Malvezzi, A. Giglia, S. Nannarone, “Determination of optical constants of scandium films in the 20-1000 eV range”, *J. Opt. Soc. Am. A* **23**, 2880-2887 (2006)
9. B. Sae-Lao, R. Soufli, “Measurements of the refractive index of Yttrium in the 50-1300 eV energy range”, *Appl. Opt.* **41**, 7309-7316 (2002).
10. T. M. Zimkina, V. A. Fomichev, S. A. Gribovskii, I. I. Zhukova, “Anomalies in the character of the x-ray absorption of rare-earth elements of the lanthanide group”, *Sov. Phys.- Sol. State* **9**, 1128-1130 (1967).
11. V. A. Fomichev, T. M. Zimkina, S. A. Gribovskii, I. I. Zhukova, “Discrete absorption by 4d electrons in the lanthanum group rare-earth metals”, *Sov. Phys.- Sol. State* **9**, 1163-1165 (1967).
12. D. W. Fischer, W. L. Baun, “Self-absorption effects in the soft x-ray M_α and M_β emission spectra of the rare earth elements”, *J. Appl. Phys.* **38**, 4830-4836 (1967).
13. B. T. Thole, G. van der Laan, and J. C. Fuggle, G. A. Sawatzky, R. C. Karnatak, J.-M. Esteve, “3d x-ray-absorption lines and the $3d^9 4f^{m+1}$ multiplets of the lanthanides”, *Phys. Rev. B* **32**, 5107-5118 (1985).
14. C. Bonnelle, R. C. Karnatak, C. K. Jørgensen, “X-ray and photoelectron spectroscopy for the determination of 4f energies of rare earths”, *Chem. Phys. Lett.* **14**, 145-149 (1972).
15. M. W. D. Mansfield, J. P. Connerade, “Observation of 4d \rightarrow f transitions in europium vapor”, *Proc. R. Soc. Lond. A* **352**, 125-139 (1976).
16. D. H. Tracy, “Photoabsorption structure in lanthanides: 5p subshell spectra of Sm I, Eu I, Dy I, Ho I, Er I, Tm I, and Yb I”, *Proc. R. Soc. Lond. A* **357**, 485-498 (1977).
17. W. E. Müller, “Optical properties of divalent rare-earthmetals and alkaline-earth metals”, *Phys. Lett.* **17**, 82-83 (1965).

18. W. E. Müller, "Optical properties of europium and barium", *Solid State Comm.* **4**, 581-583 (1966).
19. J. G. Endriz, W. E. Spicer, "Reflectance studies of Ba, Sr, Eu, and Yb", *Phys. Rev. B* **2**, 1466-1492 (1970).
20. J. F. Pétrakian, "Optical conductivity of rare-earth thin films in relation to their crystalline structure and electronic configuration", *Thin Solid Films* **38**, 83-88 (1976).
21. G. Brodén, S. B. M. Hagström, C. Norris, "UV-photoemission study of barium, europium and ytterbium", *Phy. Kondens. Materie* **15**, 327-345 (1973).
22. P. Trebbia, C. Colliex, "Study of the excitation of 4d electrons in rare-earth metals by inelastic scattering of a high energy electron beam", *Phys. Stat. Sol. (b)* **58**, 523-532 (1973).
23. G. Kaindl, G. Kalkowski, W. D. Brewer, B. Perscheid, F. Holtzberg, "M-edge x-ray absorption spectroscopy of 4f instabilities in rare-earth systems", *J. Appl. Phys.* **55**, 1910 (1984).
24. F. P. Netzer, G. Strasser, G. Rosina, "Valence excitations of rare earths by electron energy loss spectroscopy", *Surf. Sci.* **152/153**, 757-764 (1985).
25. Y. Kubo, "Self-consistent relativistic band calculations and the optical conductivities of Ba and Eu", *J. Phys. F: Met. Phys.* **16**, 585-602 (1986).
26. B.L. Henke, P. Lee, T. J. Tanaka, R. L. Shimabukuro, B. K. Fujikawa, "Low-Energy X-Ray Interaction Coefficients: Photoabsorption, Scattering, and Reflection, $E = 100-2000$ eV, $Z=1-94$ ", *At. Data Nucl. Data Tables* **27**, 1-144 (1982).
27. B.L. Henke, E.M. Gullikson, and J.C. Davis, "X-ray interactions: photoabsorption, scattering, transmission, and reflection at $E=50-30000$ eV, $Z=1-92$ ", *Atomic Data and Nuclear Data Tables* **54**, 181-342 (1993).
28. R. Verucchi, S. Nannarone, "Triode electron bombardment evaporation source for ultrahigh vacuum thin film deposition", *Rev. Sci. Instrum.* **71**, 3444-3450 (2000).

29. http://www-cxro.lbl.gov/optical_constants/
30. S. Tolansky, "Multiple-beam interferometry of surfaces and films", Oxford University Press, London, 1948.
31. L. Pasquali, A. De Luisa, S. Nannarone, "The UHV Experimental Chamber For Optical Measurements (Reflectivity and Absorption) and Angle Resolved Photoemission of the BEAR Beamline at ELETTRA", T. Warwick, J. Arthur, H.A. Padmore, J. Stöhr, eds., *AIP Conference Proceedings* **705**, 1142-1145 (2004).
32. J. A. Aznárez, J. I. Larruquert, and J. A. Méndez, "Far-ultraviolet absolute reflectometer for optical constant determination of ultrahigh vacuum prepared thin films", *Rev. Sci. Instrum.* **67**, 497-502 (1996).
33. Juan I. Larruquert, José A. Aznárez, José A. Méndez, "FUV reflectometer for in situ characterization of thin films deposited under UHV" in *Instrumentation for UV/ EUV Astronomy and Solar Missions*, Silvano Fineschi, Clarence M. Korendyke, O. H. Siegmund, and B. E. Woodgate, eds., *Proc. SPIE* **4139**, 92-101 (2000).
34. J. A. Bearden, A. F. Burr, "Reevaluation of X-ray atomic energy levels", *Rev. Mod. Phys.* **39**, 125-142 (1967).
35. C. T. Chantler, K. Olsen, R. A. Dragoset, J. Chang, A. R. Kishore, S. A. Kotochigova, D. S. Zucker, "X-Ray Form Factor, Attenuation and Scattering Tables" (version 2.1), (2005). [Online] Available: <http://physics.nist.gov/ffast> [2006, May 29]. National Institute of Standards and Technology, Gaithersburg, MD. Originally published as C. T. Chantler, *J. Phys. Chem. Ref. Data* **29**, 597-1048 (2000); and C. T. Chantler, *J. Phys. Chem. Ref. Data* **24**, 71-643 (1995).
36. M. A. Curry, S. Legvold, H. Spedding, "Electrical resistivity of europium and ytterbium", *Phys. Rev.* **117**, 953-954 (1960).

37. E. Shiles, T. Sasaki, M. Inokuti, D. Y. Smith, "Self-consistency and sum-rule tests in the Kramers-Kronig analysis of optical data: applications to aluminium", Phys. Rev. B **22**, 1612-1628 (1980).

38. Downloaded from the following web of Physical Reference Data, Physics Laboratory at NIST:
<http://physics.nist.gov/PhysRefData/FFast/Text/cover.html>.

39. M. Altarelli, D. L. Dexter, and H. M. Nussenzveig, D. Y. Smith, "Superconvergence and Sum Rules for the Optical Constants", Phys. Rev. B **6**, 4502-4509 (1972).

Table 1. Parameters used in the Drude model^a.

Drude parameters	τ_0	E_{p0}
		$7.28 \cdot 10^{-16}$ s
Coefficients	A	B
Linear	0.36	0.26
Square root	0.35	0.27

^a Parameters were made to vary in the form: $\tau(E)=\tau_0[1-A \times (E/E_0)^{(1,0.5)}]$, $E_p(E)=E_{p0}[1-B \times (E/E_0)^{(1,0.5)}]$, where the powers of 1 and 0.5 refer to linear and square root variations, respectively. $E_0=1$ eV.

Figure captions

Fig. 1. The transmittance of Eu films with various thicknesses normalized to the transmittance of the substrate *versus* the logarithm of photon energy. Solid line: 18 nm; dash-dot: 33 nm; dash-dot-dot: 55 nm; dash-dot-dot-dot: 205 nm; short dash: 24 nm; medium dash: 41 nm; long dash: 58 nm; dash-dash-dot: 57 nm; dash-dash-dot-dot: 94 nm.

Fig. 2. Log-log plot of the extinction coefficient of Eu as a function of photon energy, along with data of Henke *et al.*²⁶

Fig. 3. The extinction coefficient of Eu as a function of photon energy at the low-energy range, along with the data of Endriz and Spicer³⁵, and of Henke *et al.*²⁶

Fig. 4. The extinction coefficient of Eu *versus* photon energy at the N_{4,5} edge, along with data of Henke *et al.*²⁶

Fig. 5. The extinction coefficient of Eu *versus* photon energy at the M_{4,5} edge, along with the data of Thole *et al.*¹³ (after rescaling) and the data of Henke *et al.*²⁶

Fig. 6. Log-log plot of k data that map a wide spectral range using the current data along with the data of Endriz and Spicer³⁵, Henke *et al.*²⁶, and Chantler *et al.*³⁵, and extrapolations in the two extremes.

Fig. 7. Log-log plot of $\delta=1-n$ versus photon energy. Henke's data²⁶ are also represented

Fig. 8. n versus photon energy at the O_{2,3} edge and at the low absorption band below it. The data of Endriz and Spicer³⁵, and Henke²⁶ are also represented

Fig. 9. $\delta=1-n$ versus photon energy at the N_{4,5} edge. Henke's data²⁶ are also represented.

Fig. 10. $\delta=1-n$ versus photon energy at the M_{4,5} edge. Henke's data²⁶ are also represented.

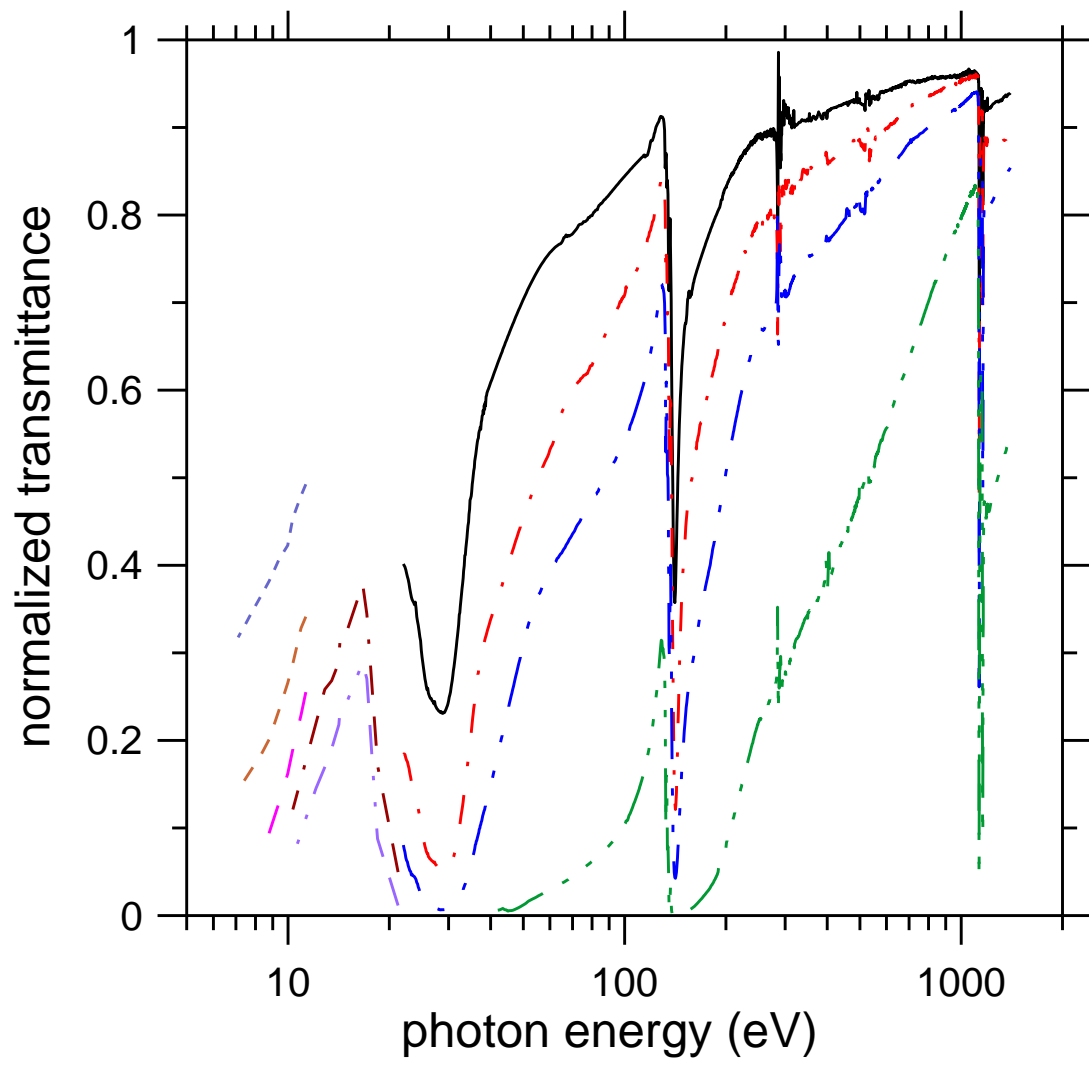


Fig 1

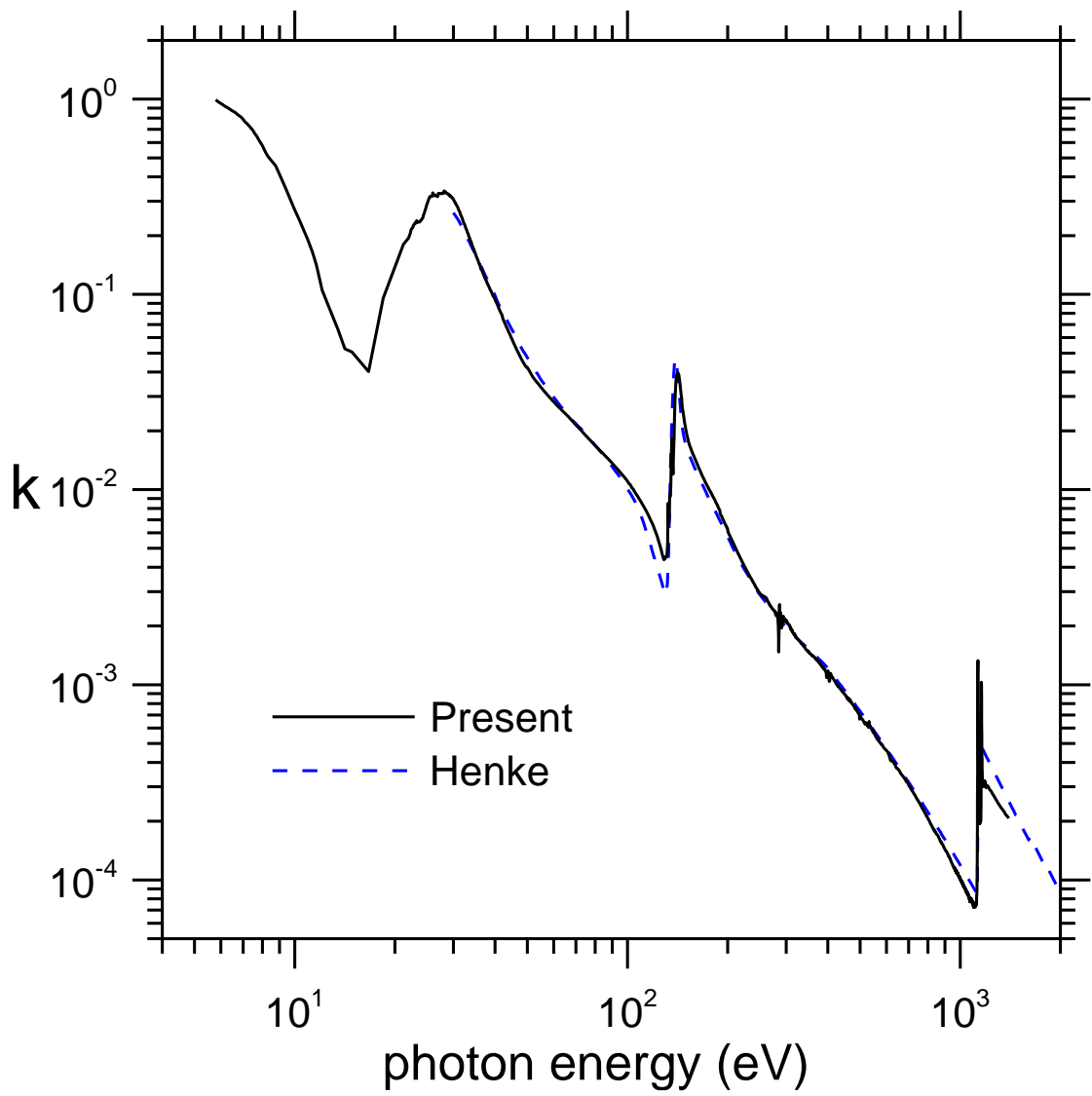


Fig 2

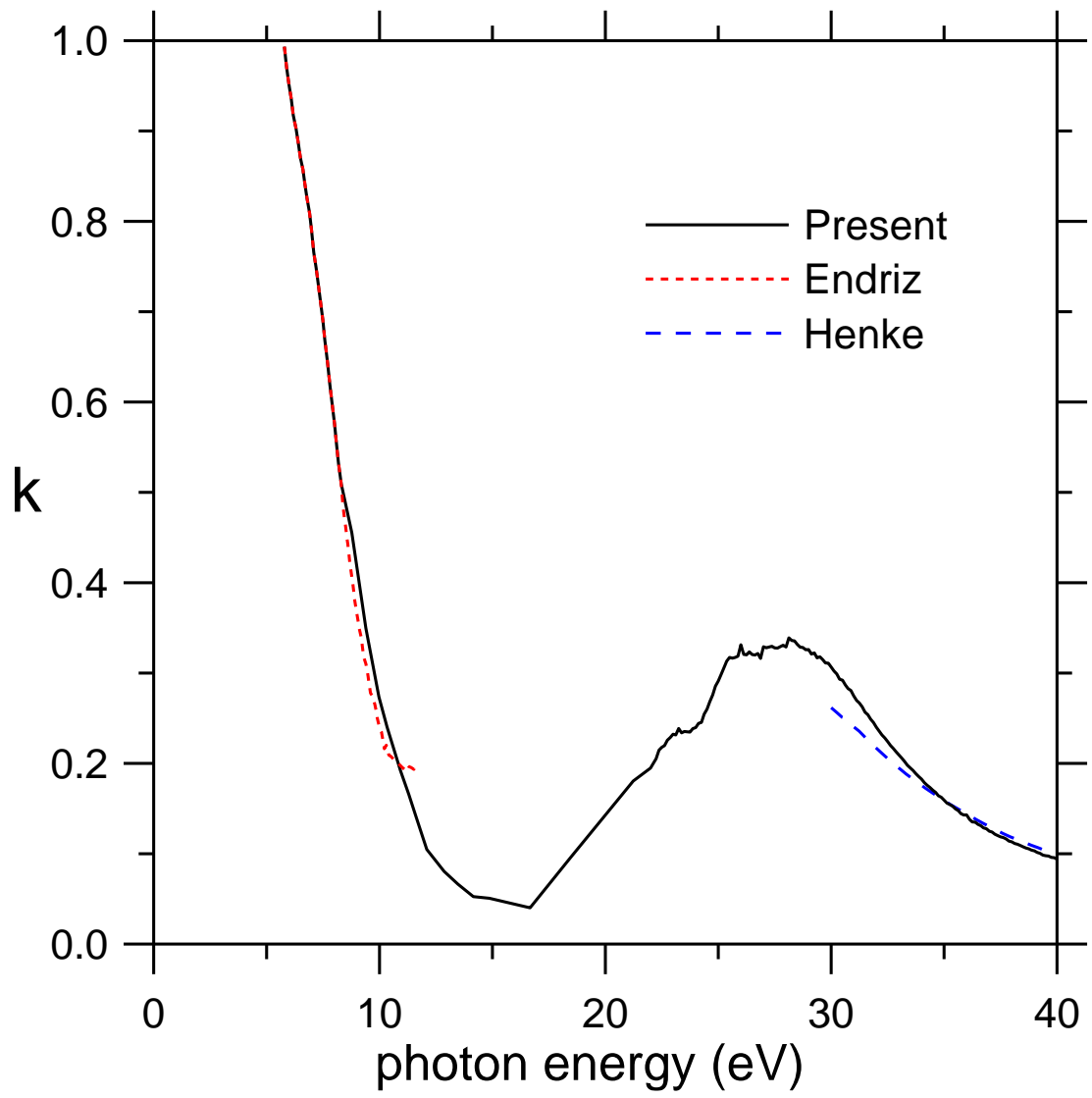


Fig 3

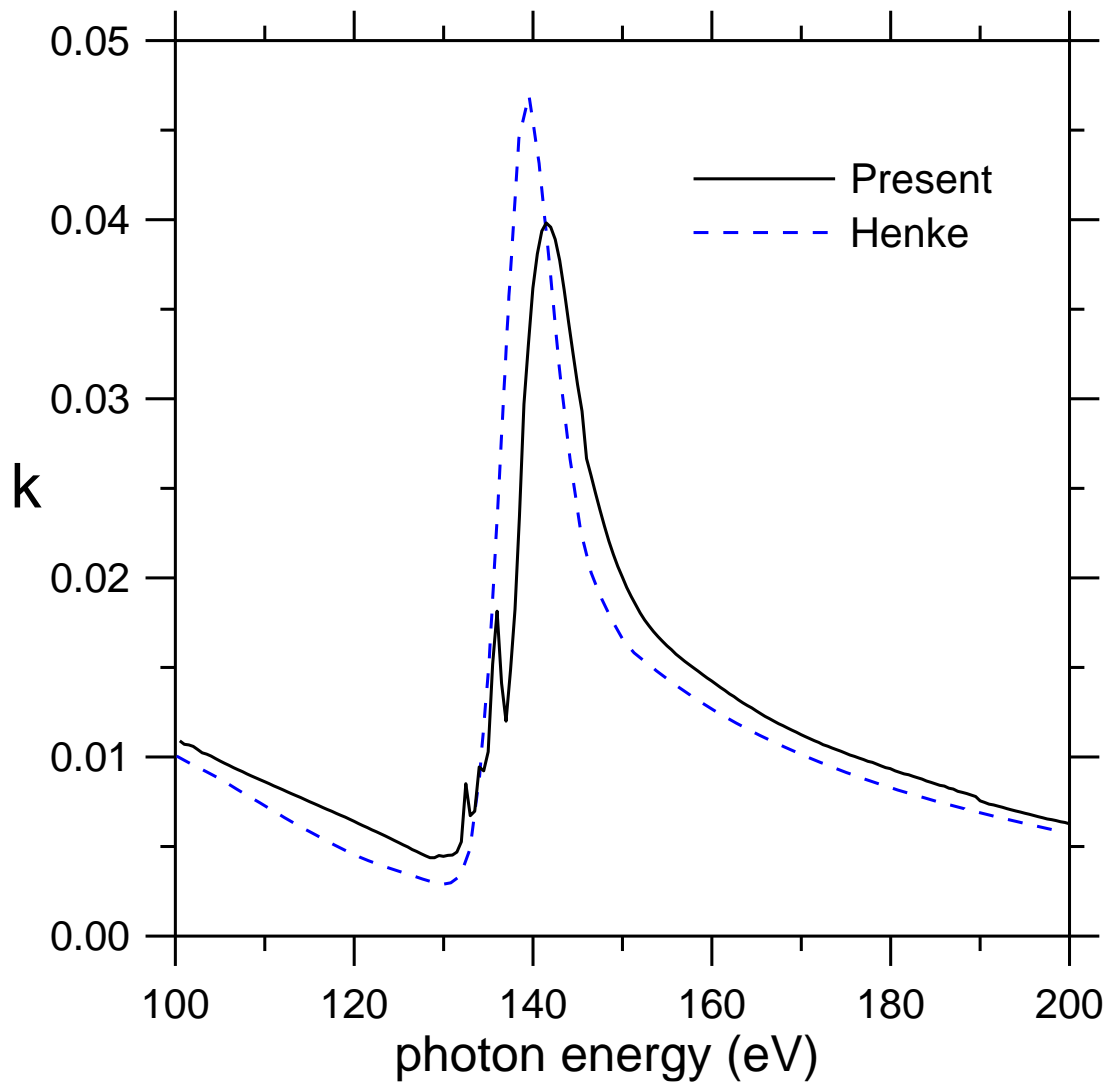


Fig 4

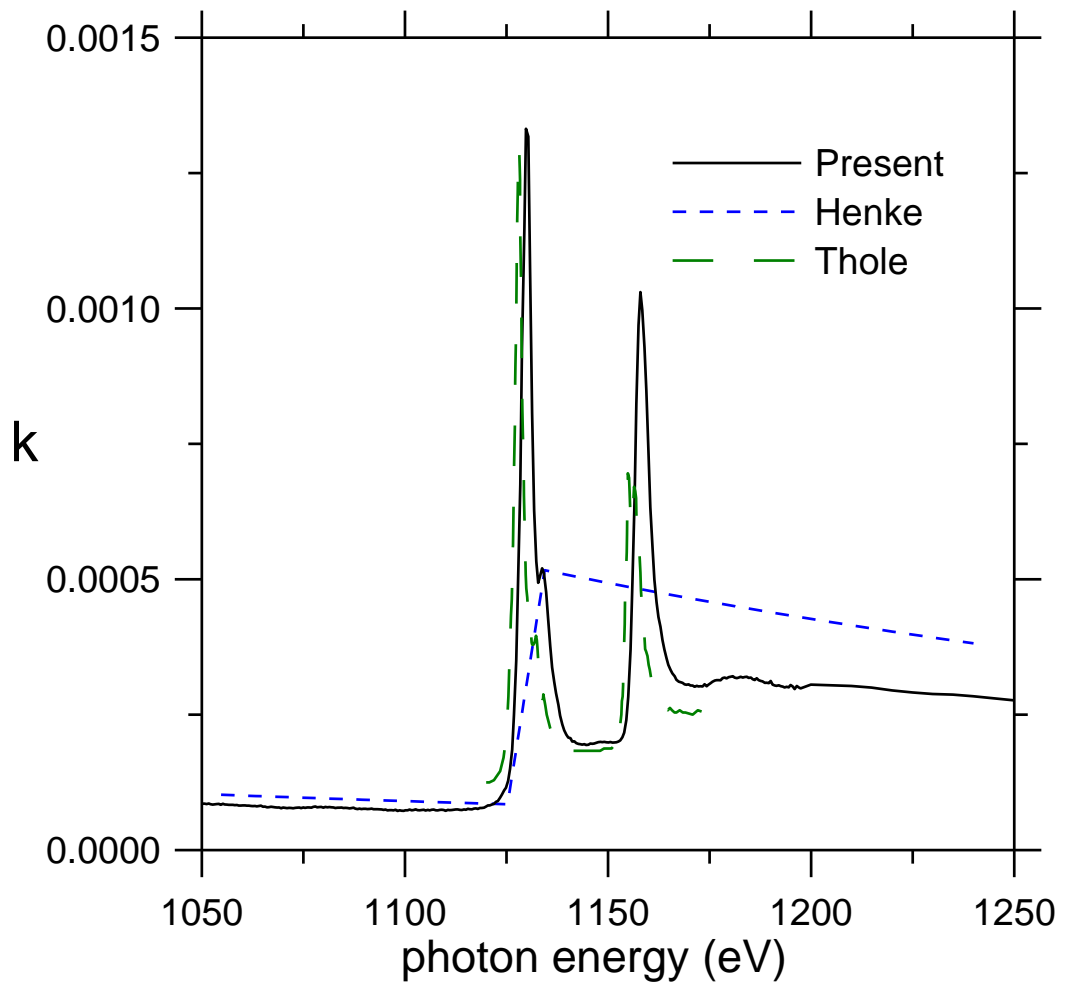


Fig 5

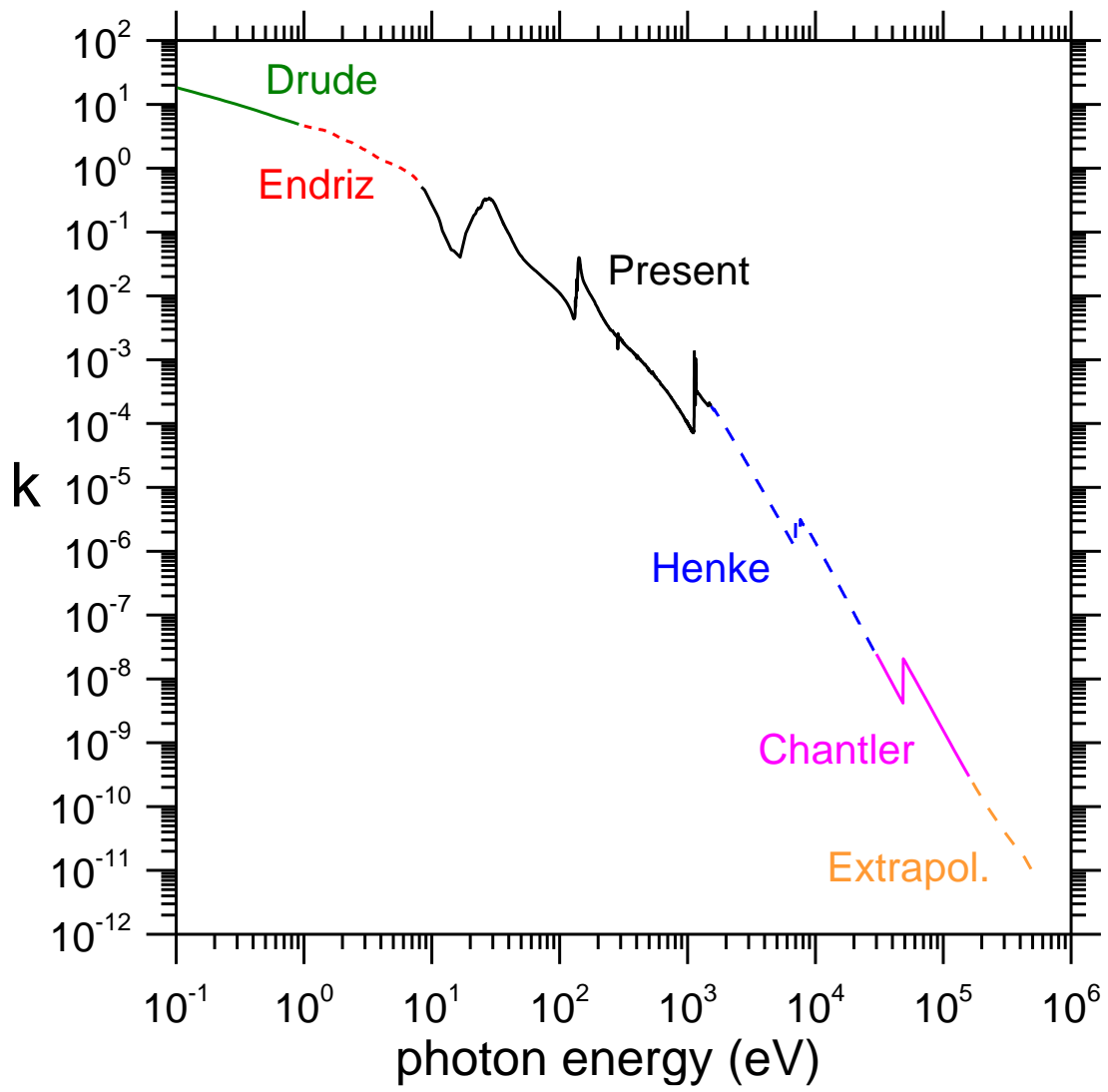


Fig 6

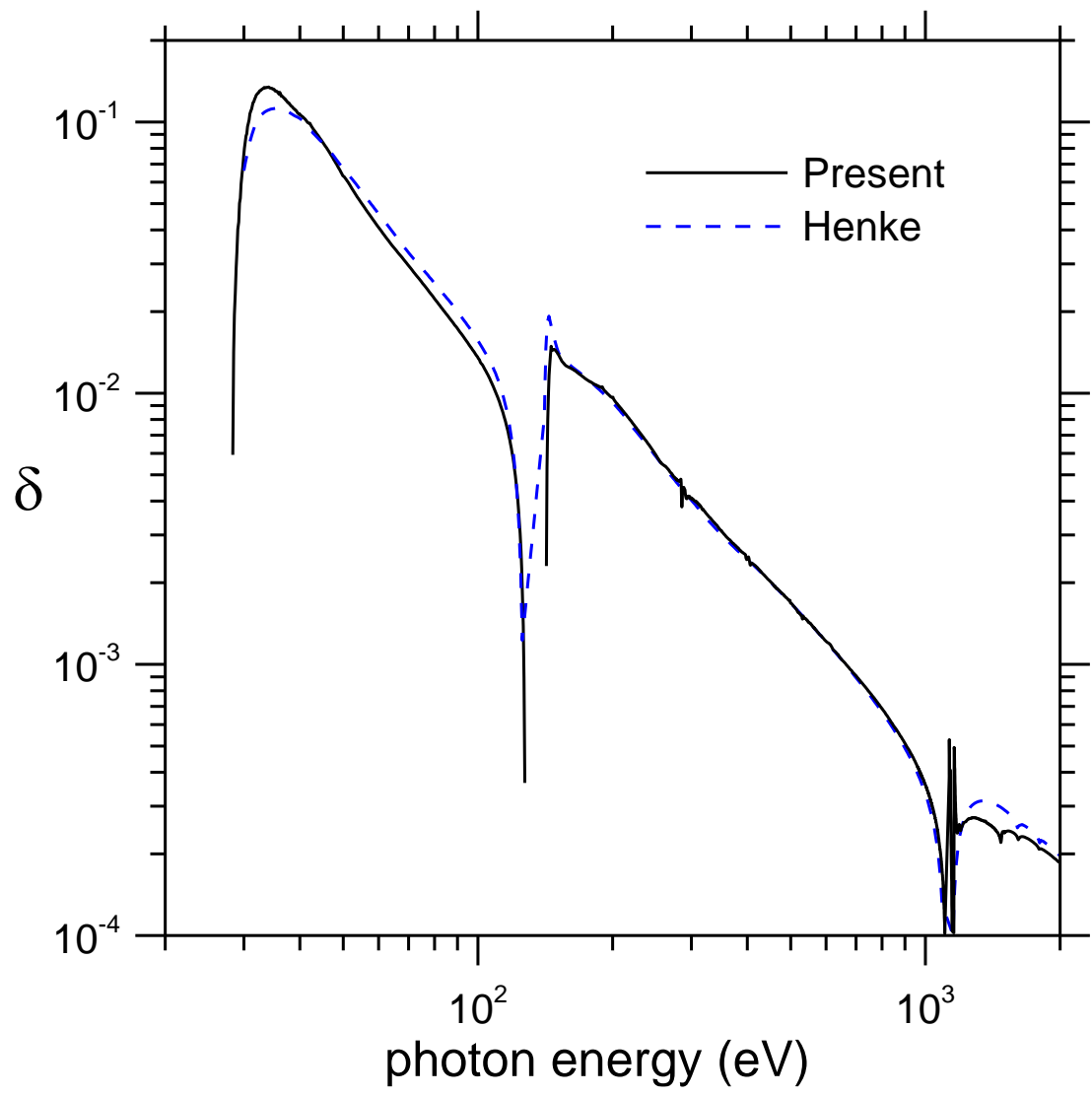


Fig 7

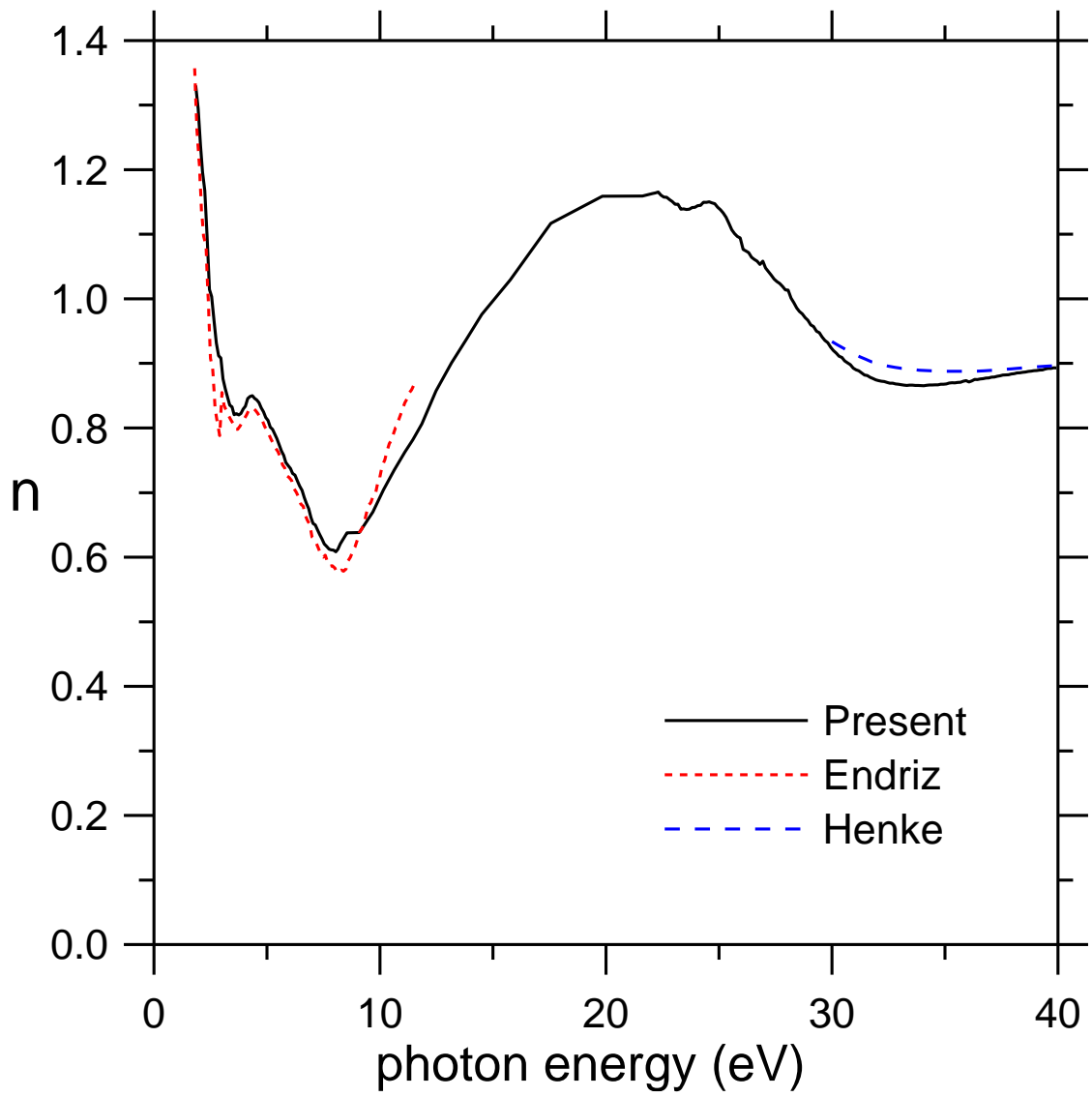


Fig 8

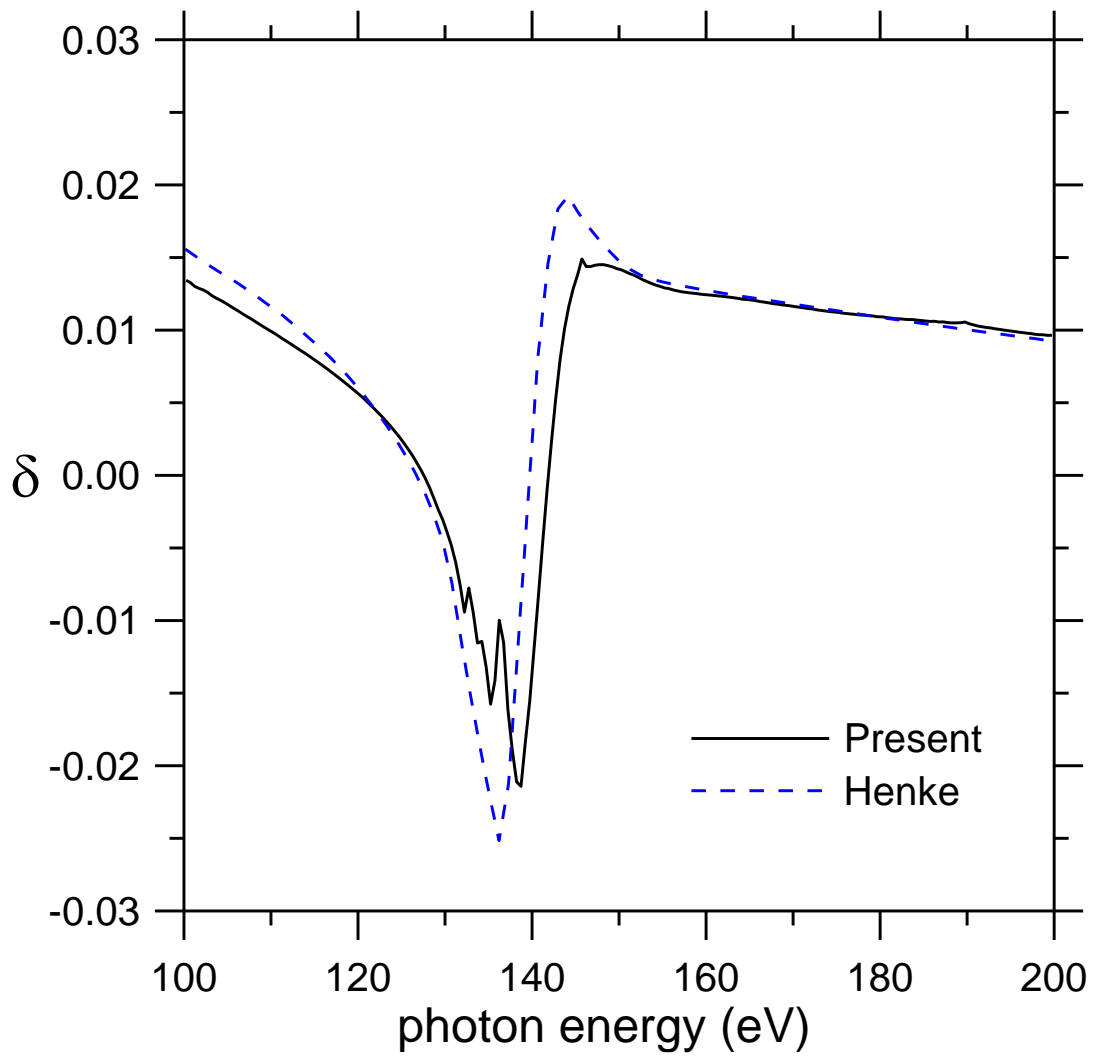


Fig 9

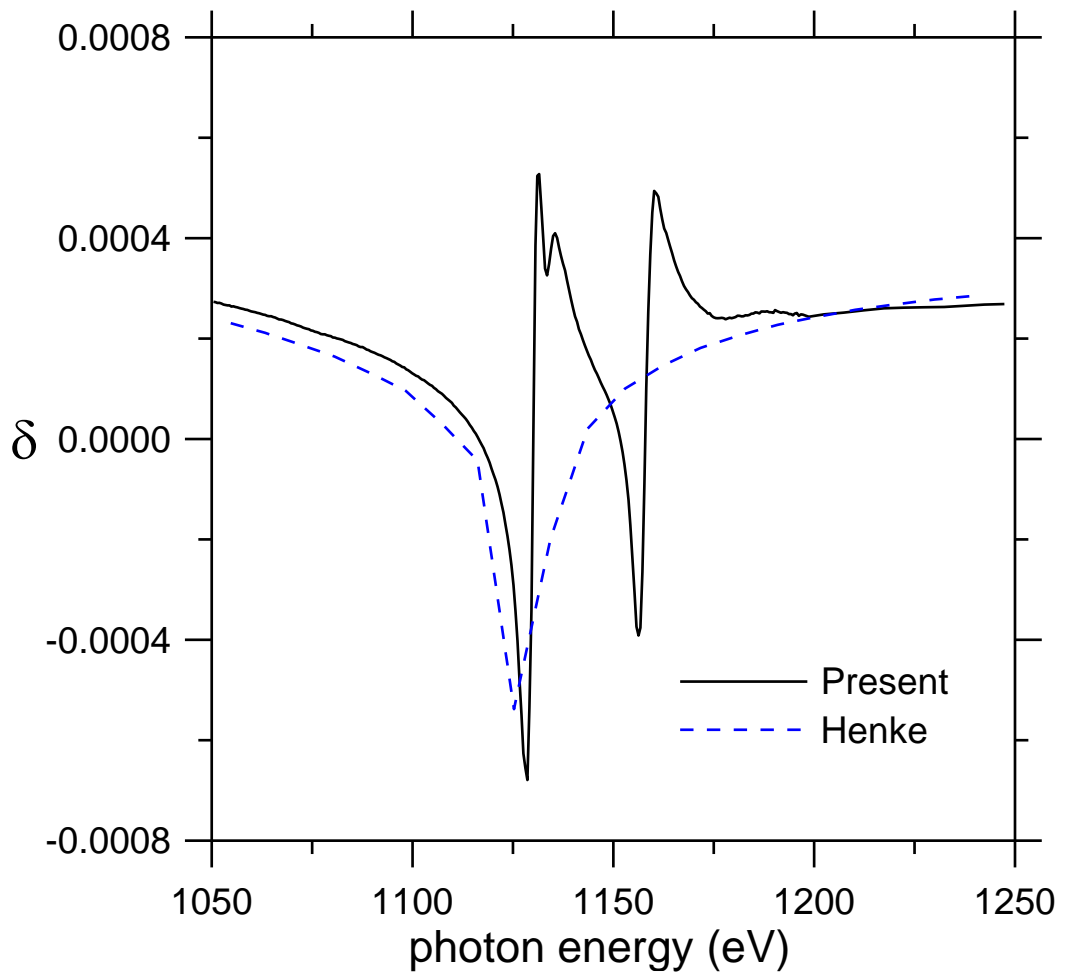


Fig 10